Pamukkale Univ Muh Bilim Derg, 31(2), 319-330, 2025

Pamukkale Üniversitesi Mühendislik Bilimleri Dergisi

Pamukkale University Journal of Engineering Sciences

Synthesis, dielectric and thermal performance of PVA nanocomposites with cadmium-based quantum dots

Kadmiyum içerikli kuantum nokta ile PVA nanokompozitlerin sentezi, dielektrik ve termal performansı

Tuna DEMİRCİ[1,3*], *Erdem ELİBOL*[2,3], *Şeref KARADENİZ*[1]

[1]Düzce University Scientific and Technological Research Application and Research Center, Düzce, Türkiye.
tunademirci@duzce.edu.tr, serefkaradeniz@duzce.edu.tr

[2]Department of Electrical-Electronics Engineering, Faculty of Engineering, Düzce University, Düzce, Türkiye.
erdemelibol@duzce.edu.tr

[3] Düzce University, Nanotechnology Research and Application Lab., Düzce, Türkiye

Received/Geliş Tarihi: 19.10.2022 Revision/Düzeltme Tarihi: 14.05.2024 doi: 10.5505/pajes.2024.85359
Accepted/Kabul Tarihi: 26.05.2024 Research Article/Araştırma Makalesi

Abstract

Hybrid polymer structures formed with semiconductor quantum dots that are doped into the polymer matrix and whose optical properties can be adjusted have attracted attention with their high usage potential in electronic applications in recent years. In this study, three types of Cd-based QD (CdX (X=Se, Te, SeTe)) were used to strengthen the poly (vinyl alcohol) (PVA) matrix and increase its optical properties. Optical, conductivity and thermal characterizations of PVA/3 different Cd-based QDs CdSe QD-PVA nanocomposites structures were evaluated comparatively. With the addition of QDs, it was observed that the PVA / QDs nanocomposites structure exhibits fluorescence properties. Hybridization structures in PVA/QDs nanocomposites structures were illuminated by FT-IR spectrum. In addition, it was determined that the thermal stability of hybrid polymer structures increased between 7-9% and the melting point of PVA/QDs hybrid polymers increased by 5-7 °C which was analyzed by DSC. The highest thermal stability and melting point increases were observed in PVA/CdSeTe QDs hybrid structures. With the addition of CdSe QDs and CdTe QDs into the PVA matrix, the conductivity value of the hybrid polymer structure increased 100 times, while the addition of CdSeTe QDs increased the conductivity by 1000 times. Similarly, in dielectric constant and dielectric loss tests, it was determined that PVA / CdSeTe QDs hybrid polymer structures are more successful than both types due to the synergic effect.

Keywords: Nanotechnology, PVA nanocomposites, Quantum dots, Optical properties, Thermal properties, Dielectric permittivity.

Öz

Polimer matrisine katkılı yarı iletken kuantum noktaları ile oluşturulan ve optik özellikleri ayarlanabilen hibrit polimer yapıları, son yıllarda elektronik uygulamalarda yüksek kullanım potansiyelleri ile dikkat çekmektedir. Bu çalışmada, poli(vinilalkol) (PVA) matrisini güçlendirmek ve optik özelliklerini arttırmak için üç tip Cd bazlı kuantum nokta (QDs) (CdX (X=Se, Te, SeTe)) kullanılmıştır. PVA/3 farklı Cd tabanlı QDs yapılarının optik, iletkenlik ve termal karakterizasyonları karşılaştırmalı olarak değerlendirildi. QDs'lerin eklenmesiyle birlikte PVA/QDs nanokompozit yapısının floresans özellikleri sergilediği gözlemlendi. PVA/QDs nanokompozit yapılarındaki hibridizasyon yapıları FT-IR spektrumu ile aydınlatılmıştır. Ayrıca DSC ile analiz edilen hibrit polimer yapıların termal stabilitesinin %7-9 arasında arttığı ve PVA/QDs hibrit polimerlerin erime noktasının 5 ile 7 °C arttığı tespit edilmiştir. En yüksek termal kararlılık ve erime noktası artışları PVA/CdSeTe QDs hibrit yapılarında gözlendi. PVA matrisine CdSe QDs'ler ve CdTe QDs'lerin eklenmesiyle hibrit polimer yapısının iletkenlik değeri 100 kat artarken, CdSeTe QDs'lerin eklenmesi iletkenliği 1000 kat artırmıştır. Benzer şekilde dielektrik sabiti ve dielektrik kayıp testlerinde de PVA/CdSeTe QDs hibrit polimer yapılarının sinerjik etki nedeniyle her iki tipe göre daha başarılı olduğu tespit edilmiştir.

Anahtar kelimeler: Nanoteknoloji, PVA nanokompozitleri, Kuantum noktaları, Optik özellikler, Termal özellikler, Dielektrik geçirgenlik.

1 Introduction

Since the 2000s, nanoparticles have become the center of attention of many researchers with their desired size, shape and highly efficient synthesis properties. Semiconductor nanoparticles are semiconductor nanoparticles known as quantum confinement (QD), which are under the influence of quantum confinement in three dimensions and whose optical and electrical properties can vary depending on their size [1]. QDs are semiconductor nanoparticles used in many optical systems due to their fluorescence effect, tunable energy band structure and low cost. These nanoparticles used in optical systems have two main skeletons, II-IV and III-V. The most well-known members of these systems are CdX (X=S, Se, Te) [2]. Cd-based QDs, first synthesized in 1993, are a member of the II-IV group and find use in many different applications. For example, CdX (X=SeTe, Se, Te) has been successfully used in many fields including the development of electronic devices [3], solar cells [4], electrogenerated chemiluminescence [5], biological applications [6] and composite technology [7],[8]. With the introduction of QDs in nanocomposite technology in recent years, it has become extremely important to improve the performance of devices containing polymer structures and to gain new application areas with this development.

Especially in recent years, QDs have been used in polyvinylpyrrolidone (PVP) [9], polyamide (PA) [8]-[10], poly (9,9-di-n-octylfluorenyl-2,7-diyl (PFO) [11], polyvinyl alcohol (PVA)[12].], polyvinyl alcohol (PVA) [12] has been frequently used in the literature and has been successfully applied in this regard. Polyvinyl alcohol is one of the most widely used hydrophobic polymer types for thin film preparation. This is due to the presence of free hydroxyl (OH) groups in its structure. The presence of OH groups in the side chains of the

*Corresponding author/Yazışılan Yazar

PVA structure allows them to interact easily with II-IV type nanoparticles [13]. Cadmium-based QDs with II-IV properties have been shown to provide significant contributions to PVA thin films such as thermal counteraction, degradation, fluorescence contribution, and enhancement of optical and electronic properties. The most basic examples of these are nanocomposite Schottky diodes [14], UV blockers in food packaging [15] and protein scavengers [16]. It has been shown in previous studies that CdSe and CdTe QDs, which form hybrid structures with polymer structures, are effective in increasing the conductivity, hardness and fluorescence properties of the polymer structure [12],[17],[18]. On the other hand, alloy CdSeTe QDs [19], which have been used in many applications in the literature in recent years and whose energy band gaps can be tuned more precisely thanks to their alloy structure, are utilized in hybrid form with polymer structures.

Poly (vinyl alcohol) (PVA) is a synthetic polymer widely used in a variety of applications due to its excellent film-forming and adhesive properties as well as its biocompatibility. PVA is a water-soluble polymer that can form transparent films when dried, useful in applications such as coatings, adhesives, textiles and packaging materials [20].

A common method for crosslinking PVA is the use of chemical crosslinkers such as glutaraldehyde, formaldehyde or borax. These crosslinkers react with the hydroxyl groups (-OH) present in PVA molecules to form covalent bonds between the polymer chains. The introduction of quantum dots can be achieved by mixing with the PVA solution before the crosslinking reaction takes place. The quantum dots are incorporated into the PVA matrix during the crosslinking process. Anot her approach to incorporate quantum dots into PVA is physical crosslinking. Physical crosslinking involves the use of external stimuli such as heat, UV radiation or a combination of both to induce crosslinking of the polymer chains [21].

In this study, water-based alloy CdSeTe QDs, synthesized for the first time in the literature, were added to the PVA matrix and PVA/CdSeTe QD nanocomposite structures were obtained. In order to make a comprehensive comparison depending on the QD type, three different Cd-based QDs (CdSe, CdTe, CdSeTe) were added to the PVA matrix and optical, conductivity and thermal characterizations of PVA/CdX (X=Se, Te, SeTe) were performed so that the molarities of the three QDs and the thicknesses of the PVA/QDs nanocomposites were completely equal to each other during the study. The morphological, thermal, optical, photoluminescence and electrical properties of the N-type hybrid polymer nanocomposites were investigated and comparative analysis was performed according to the type of QDs used.

2 Material and methods

2.1 Material

PVA (Mw~8000) and all chemicals were purchased Sigma-Aldrich and used directly without any purifications. Deionized water was produced through a Thermo Scientific purification system (≥18 MΩ,) special.

2.2 Synthesis

2.2.1 Preparation methods of precursor solutions

Preparation of cadmium precursor solution; 0.146 g cadmium chloride ($CdCl_2$, 0.8 mmol) was dissolved in 160 ml ultra-pure water and 118.5 µL 3-mercapto propionic acid (MPA) ($HSCH_2CH_2CO_2H$) was added to the solution. When the mixture becomes homogeneous, the pH was adjusted to 12 with 0.1 M sodium hydroxide (NaOH) [22].

2.2.2 Preparation of selenium precursor solution

0.021 g of selenium powder (Se, 0.4 mmol) and 0.038 g of sodium borohydride ($NaBH_4$, 1 mmol) were taken into a double neck reaction flask and 10 mL of ultra-pure water was added to the mixture. The solution was stirred for 30 min at 80 °C in an inert environment [22].

2.2.3 Preparation of tellurium precursor solution

0.051 g of tellurium powder (Te, 0.4 mmol) and 0.038 g of sodium borohydride ($NaBH_4$, 1 mmol) were taken into a double-necked reaction flask and 10 mL of ultrapure water was added. This mixture was stirred for 30 minutes at 80 °C in an inert environment.

2.2.4 Preparation of CdSe QDs

After the precursors were ready, 2.0 ml of the Se precursor was quickly injected into 50.0 mL of the Cd precursor. The solution was kept at 80 °C for 15 min. for the growth of CdSe QDs. The solution temperature was then lowered to room temperature with the aid of an ice bath. The CdSe QD solution was washed with ethanol: acetone at a ratio of 1:1 and centrifuged for 3 rounds to be purified. Then, the CdSe QDs obtained in solid form were dissolved in ultrapure water and the pH value was adjusted to 10 for use with 0.1 M sodium hydroxide (NaOH) [22].

2.2.5 Preparation of CdTe QDs

To synthesize CdTe QDs, 2.0 ml of Te precursor was injected quickly with the help of a syringe into the Cd precursor, which was ready at 80 °C an inert medium. The solution was stirred at 80 °C for 15 min. and then cooled rapidly with an ice bath. Similarly, in the purification of CdTe QDs, the solution was centrifuged after washing with ethanol: acetone. Then CdTe QDs were re-dissolved in ultrapure water and adjusted to pH=10 [23].

2.2.6 Preparation of CdSeTe QDs

For the water-based synthesis of CdSeTe QDs, firstly, 1.0 ml of Se precursor was injected into 50.0 ml of Cd precursor kept at 80 °C in an inert environment and the mixture was kept at this temperature for 10 min. Then, 1.0 ml of Te precursor was injected into the mixture and the solution was continued to be stirred at 80 °C for another 10 min. The solution was then cooled to room temperature and washed with ethanol: acetone mixture and centrifuged to purify the CdSeTe QDs. The CdSeTe QDs, like other QDs, were dissolved in ultrapure water and the pH was adjusted to 10 and ready for use [24].

2.2.7 Preparation of PVA (m/V)

10 g of PVA was dissolved in 100 ml of ultrapure water and stirred at 65 °C for 30 min. After obtaining a homogeneous structure, the mixture was poured into a glass layer and kept at room temperature in a vacuum oven for 3 days.

2.2.8 PVA/CdX (X=Se, Te, SeTe) QD nanocomposites

To obtain PVA/CdX (X = Se, Te, SeTe) QD CdSe QD-PVA nanocomposites structures, firstly 10 g of PVA was dissolved in 100 ml of ultrapure water at 65 °C. The mixture was stirred for 30 min. at this temperature and a homogeneous structure was

obtained.
In order to obtain 3 different PVA/CdX (X=Se, Te, SeTe) QD thin film, 10.0 ml of PVA solutions were divided into 3 different beakers. 1.0 ml of CdSe QD, 1.0 ml of CdTe QD and 1.0 ml of CdSeTe QD solutions were separately injected into 3 different PVA solutions to obtain PVA: QD rate as 10:1. The mixtures were continued to be stirred at 65 °C for another 30 minutes and the QD's were homogeneously dispersed in the PVA matrix. The solvents were then poured into glass plates and allowed to dry in a vacuum oven for 3 days.

3 Results and discussion

3.1 Structural Analysis

The structural characterizations of PVA/QD' nanocomposites prepared during the study were demonstrated in micrographs using Quanta FEG 250 SEM. SEM images obtained for PVA and PVA/QDs are given in Figure 1. In Figure 1(a), the SEM image of pure PVA nanocomposites is given and the homogeneity of the surface is seen. On the other hand, with the QDs added to the surface, although the QDs are homogeneously distributed on the surfaces, some roughness is noticeable. EDAX analysis was performed to determine the number of molecules on the PVA/QDs surfaces. The PVA/QDs thin film showed 1.06 % Cd and 0.86 % Se for CdSe QDs, 1.96 % Cd and 1.09 % Te for CdTe QDs, 1.22 % Cd, 1.13 % Te and 1.06 % Se for CdSeTe QDs. PVA measurements are indicated with an average of 55 % C and 42 % O. Figure 2 shows the AFM images of PVA, CdSe QDs-PVA, CdTe QDs-PVA and CdSeTe QDs-PVA nanocomposites taken at room temperature, respectively. As shown in Figure 2, the roughness structure of the surface morphology of the designed PVA and PVA-QDs nanocomposite structures was investigated and it was found that there are quantum dots in clusters in PVA to provide the optimal surface energy. This resulted in the nanocomposite structure of PVA-based QDs having a wavy appearance. The average surface roughness (RMS) and average roughness values of the thin films were 18.00 nm, 5.79 nm and 13.98 nm for PVA/CdSe QDs, PVA/CdTe QDs and PVA/CdSeTe QDs, respectively.

In the study, XRD analysis was performed to determine the crystal structure of PVA / QDs nanocomposites and compared with conventional XRD analysis of pure PVA. RIGAKU Smart lab device was used for XRD analysis. It is known that the main peak of the XRD pattern of PVA is 20° [25]. This crystal structure of PVA has been realized thanks to the hydrogen bond interactions in the molecule. It is known that the 3 different QDs used in this study have a zinc cubic blend structure. The XRD peaks obtained in the studies in the literature for these three QD types can be listed as follows; XRD peaks of CdSe QDs are 2Θ=24° (111) and 2Θ = 39° (311) [1] XRD peaks for CdTe QDs are 2Θ=24° (111), 2Θ = 39° (220) and 2Θ=46° (331) [26] and XRD peaks of CdSeTe QDs are 2Θ=24° (111), 2Θ = 41° (220) and 2Θ = 48° (311) [27].

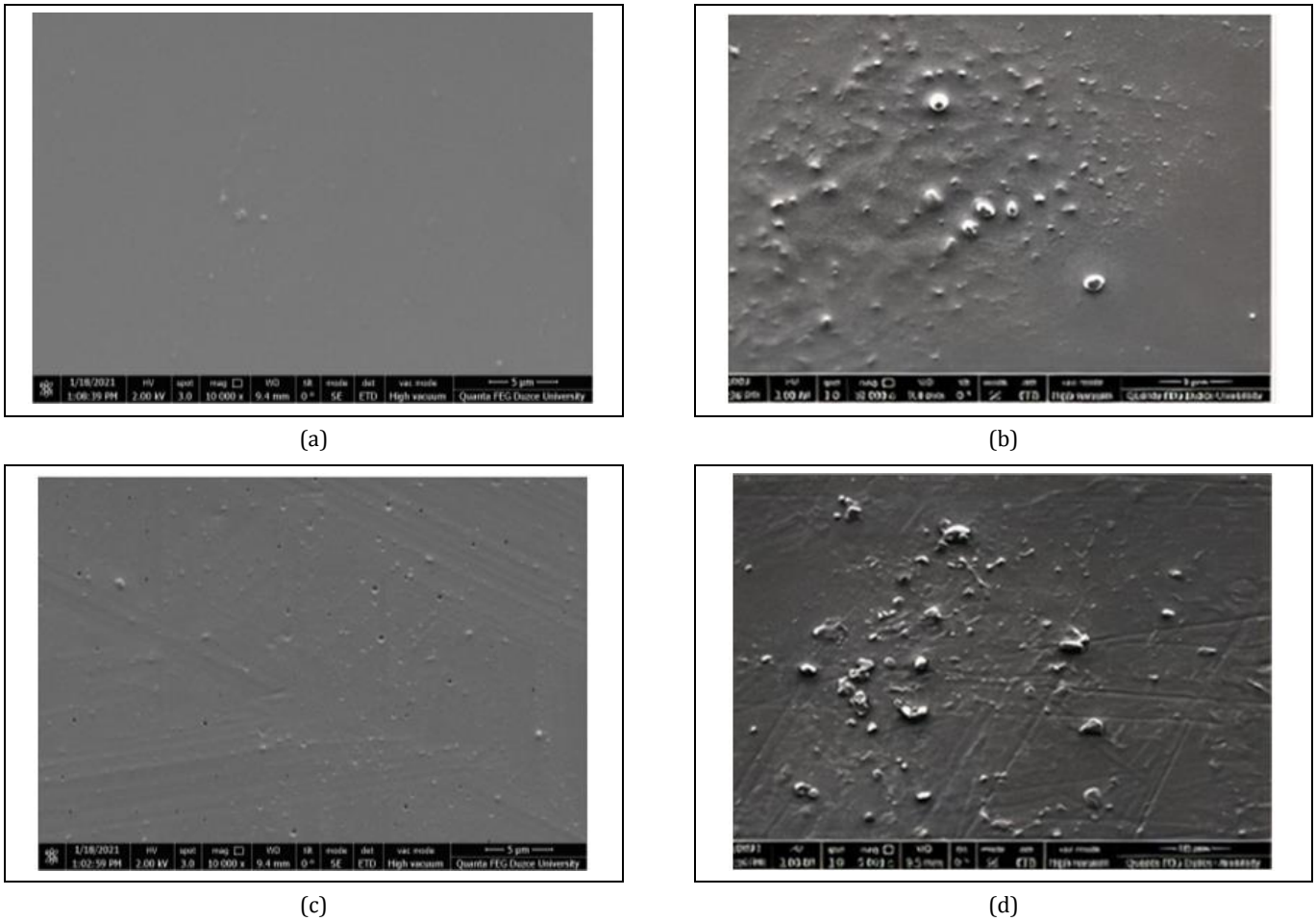

(a) (b) (c) (d)

Figure 1. SEM micrographs of (a): PVA. (b): CdSe-PVA. (c): CdTe QDs-PVA. (d): CdSeTe QDs-PVA.

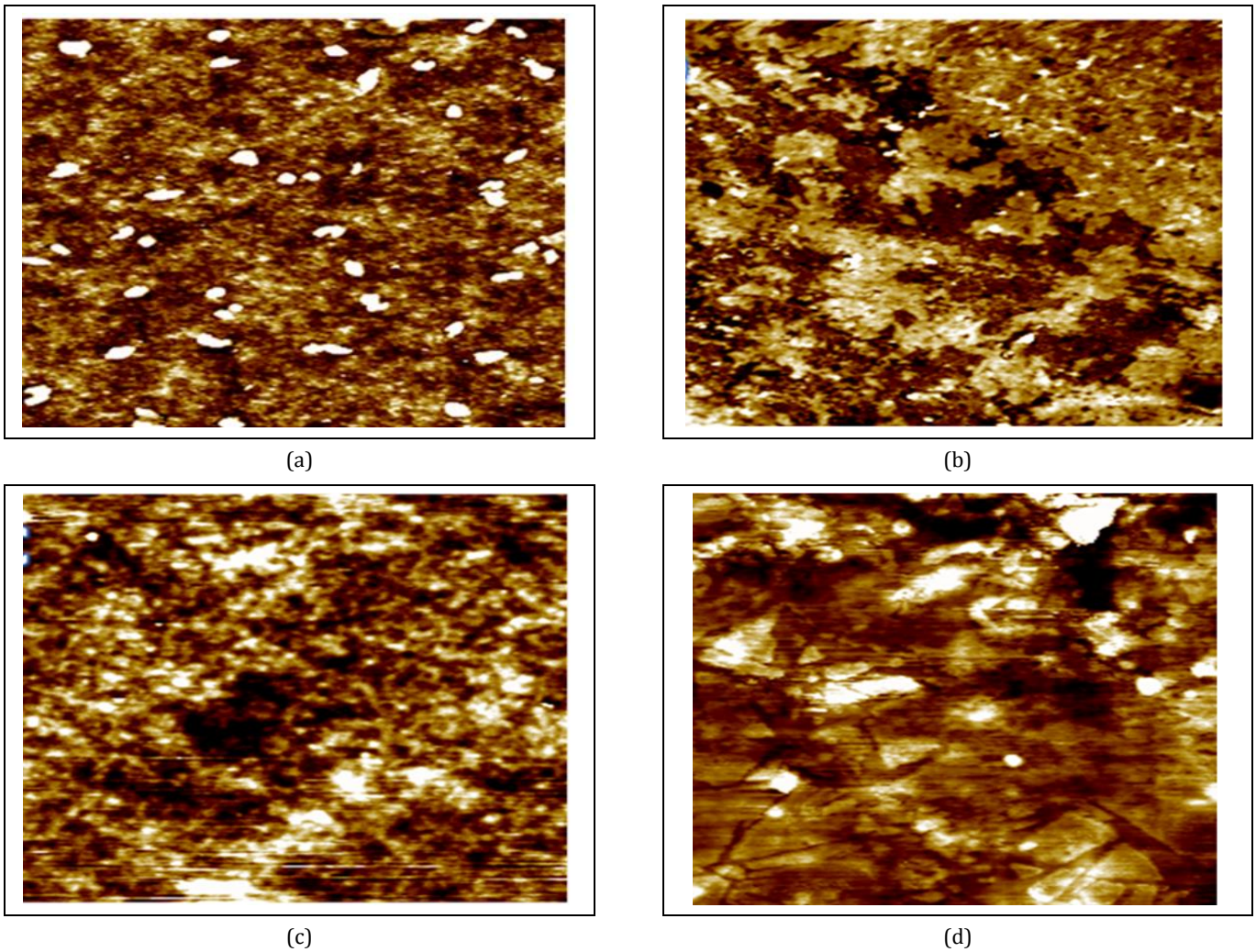

(a) (b)

(c) (d)

Figure 2. AFM micrographs of (a): PVA. (b): CdSe QDs-PVA. (c): CdTe QDs-PVA. (d): CdSeTe QDs-PVA.

XRD analyses were performed for 3 different PVA/QD surfaces prepared in this study and the results obtained are shown in Figure 3. Figure 3(a) shows the XRD results of the PVA/QD nanocomposite structure and the results are compared with the JCPDS standard results. As can be seen in Figure 3, due to the limited amount of CdSe QD in PVA, the peak at approximately 26° (111) shown in the CdSe JCDPS (No: 00-019-0191) standards, the peak at 42.5° (200) was at low power, while the peak at 49 ° (311) became too small to be detected. In the JCPDS standards, the structure of the PVA/CdSe QDs surfaces appears as a zinc cubic blend structure. Figure 3(b) shares the XRD characterization results obtained for PVA/CdTe QDs nanocomposites. CdTe QDs JCPDS (No.65-1046) was used here for comparison. In the XRD patterns of PVA/CdTe QDs nanocomposites, the first peak appeared as a neck next to the PVA peak, while the peaks at 42° (220) and 48° (311) were more prominent compared to PVA/CdSe QDs nanocomposites. Again, Figure 3(c) shows the XRD characterization results of PVA/CdSeTe QDs. Due to the alloy structure of CdSeTe QDs, JCPDS standards of both CdSe QDs and CdTe QDs were used for XRD characterization. PVA/CdSeTe QDs were also not detected in thin films due to the low strength of the third peak. Although this is thought to be mainly due to the low amount of QDs on the surface, it was observed that the peaks of Te^{2+} QDs were stronger than those of Se^{2-} QDs.

The thermal properties of PVA/CdX QDs nanocomposites were investigated in nitrogen environment in the range of 25-650 °C at 20 °C/min using Shimadzu TA-60 instrument. Thermogram analyses, thermogravimetric and differential thermal analysis (TG-DTA) results due to the interaction between CdSe QDs, CdTe QDs and CdSeTe QDs and PVA are shown in Table 1 and Figure 4.

When the PVA/QDs structures were examined, it was observed that the water and volatile molecules in the structure were firstly separated up to 190 °C. The second fragmentation period in the TG-DTA graphs corresponds to the half-chain breaks of the PVA structure and lasts up to 405 °C. In this range, an average 12-13 % increase in crosslinking reactions was observed with the presence of QDs in the PVA structure, regardless of the type of QD. The main reason for this increase is thought to be due to the strengthening of the CdSe QDs-PVA nanocomposite structure by chemical interactions (Van Der Waals) between carboxylic acids and QDs in the structure of PVA.

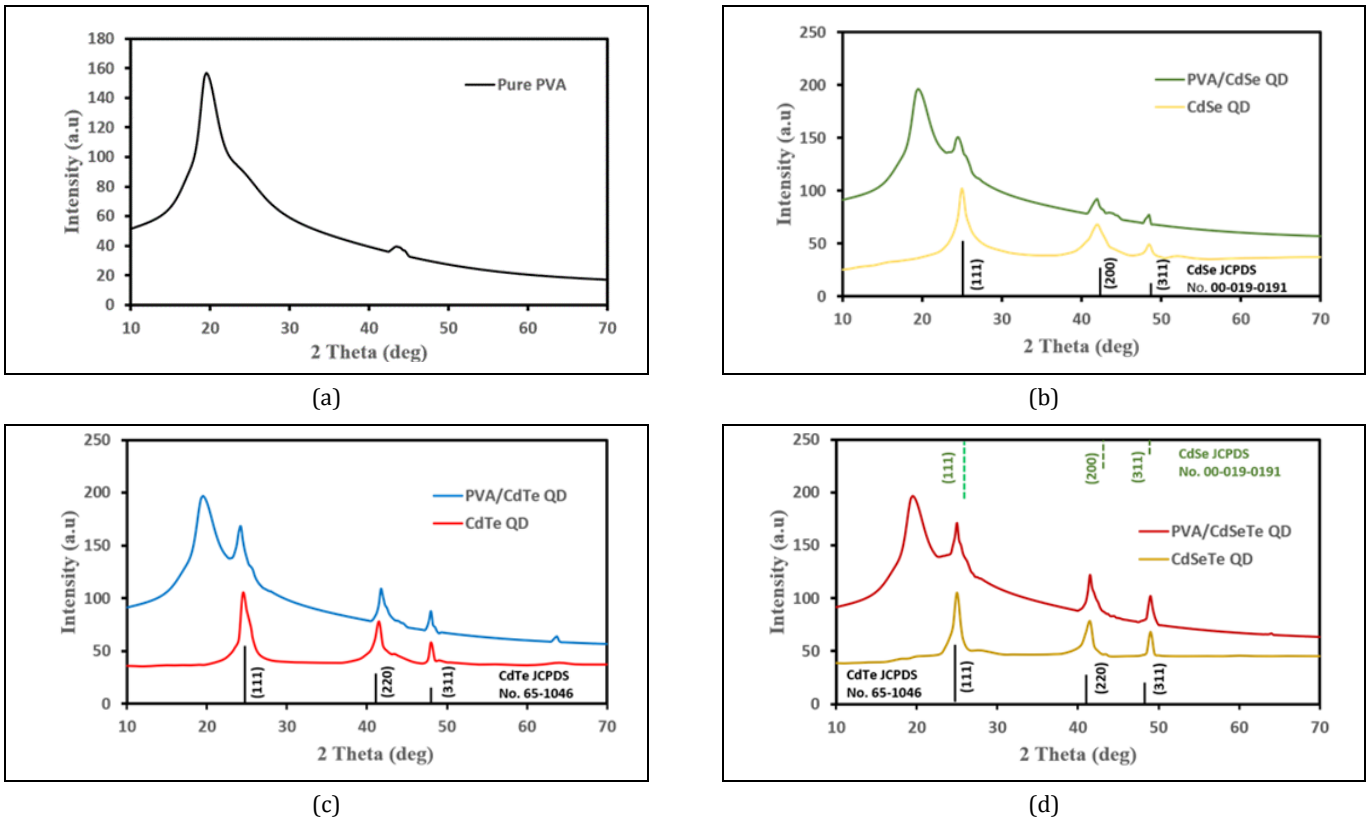

Figure 3. XRD spectrum of Cd based QDs-PVA nanocomposites.

Table 1. Thermal Decomposition of PVA and QDs-PVA nanocomposites.

Temperature(°C)	<190	190-405	405-600	Ash
		Weight Loss (%)		
PVA	7.67	70.11	22.22	0.00
PVA-CdSe QDs	7.25	60.23	30.92	1.60
PVA-CdTe QDs	7.87	54.04	35.11	2.98
PVA-CdSeTe QDs	7.11	54.90	34.74	3.25

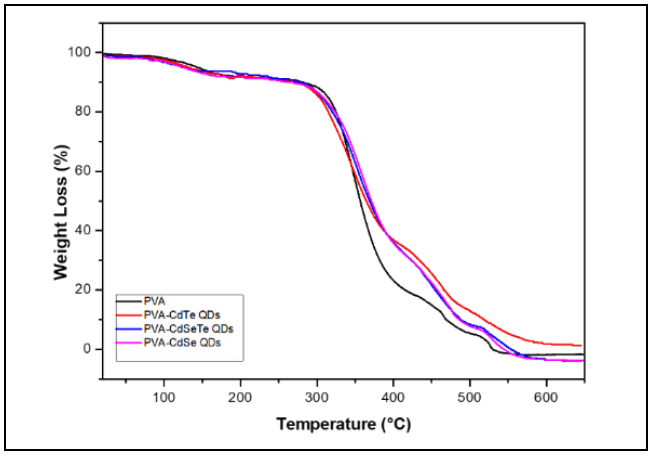

Figure 4. TGA Spectrum of PVA and QDs-PVA nanocomposites.

While no major differences were observed between the surfaces in the first two thermal breakdown periods, differences were observed in the 480 °C and 650 °C ranges depending on the QD used in the third thermal breakdown period shown in Table 1. The third thermal breakdown observed between 480 °C and 650 °C was 22.22 % for pure PVA nanocomposites, 30.92 % for PVA/CdSe QDs nanocomposites, 35.11 % for PVA/CdTe QDs nanocomposites and 34.74% for PVA/CdSeTe QDs nanocomposites. Considering the secondary and tertiary thermal breakdown values, it is concluded that QDs increase the thermal stability of the PVA nanocomposite structure. This increase was found to be 7.06%, 6.29% and 9.25% (m/m) for CdSe QD, CdTe QD and CdSeTe QD, respectively. When the remaining part of the combustion was examined, it was found that CdSe QDs-PVA was 1.60 %, CdTe QDs-PVA was 2.98 %, and CdSeTe QDs-PVA was 3.25 %. These values showed the % elemental part (Cd, Se, Te) in PVA. This value showed linear results with SEM-EDAX.

The characterization of the hybrid polymer QDs-PVA nanocomposites obtained by adding cadmium-based quantum dots to PVA was investigated by DSC. The DSC characterization curves obtained are shown in Figure 5 and the parameter values obtained from these curves are shown in Table 2. When the DSC diagram shown in Figure 5 is examined, large peaks around 120 °C were observed in PVA and PVA/QDs nanocomposite structures. İndicating the presence of water in the structures. The peaks between 190-200 °C, which appear more pronounced than this peak, indicate the melting point of PVA nanocomposites and PVA/QDs nanocomposites.

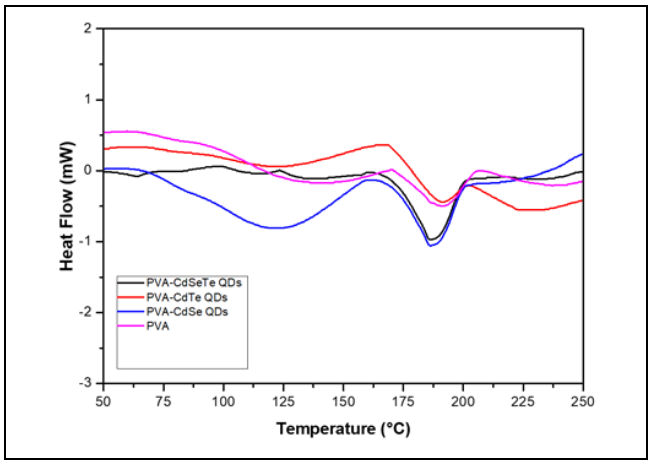

Figure 5. DSC Spectrum of QDs-PVA nanocomposites.

Table 2. PVA and QDs-PVA nanocomposites T_m point.

	Tm (°C)	Delta Hf (j/g)
PVA	191.16	20.65
PVA-CdSe QDs	192.57	21.97
PVA-CdTe QDs	194.97	23.13
PVA-CdSeTe QDs	198.23	26.17

When the changes in the melting points of nanocomposites due to the addition of QDs to the PVA matrix are examined, it is seen that while the melting point for PVA is 191.16 °C, this value increases to 192.5 °C for PVA/ CdSe QDs, 194.97 °C for PVA/CdTe QDs and 198.23 °C for PVA/CdSeTe QDs. Thus, it was clearly seen with the results obtained that the QDs added to the PVA matrix increased the melting point of the QDs-PVA nanocomposite structure. It was determined that the highest increase in this melting point was obtained by adding CdSeTe QDs with a value of 7.07 °C. In addition, when the crystallization rates were examined, it was observed that the crystallization increased by 1.23 %, 0.98% and 3.45 % with the addition of CdSe QDs, CdTe QDs and CdSeTe QDs, respectively, compared to pure PVA nanocomposites.

FTIR Spectra analyses of PVA/CdX QDs nanocomposites were measured on Shimadzu IR Prestige-21 using ATR apparatus. FTIR reviews were carried out in thirty-two scans. The FTIR spectra of CdSe, CdTe QDs and CdSeTe QDs showed aliphatic C-H vibrations at 2950 cm^{-1} [26] and 2899 cm^{-1} [27]. Again, C=O peaks of carboxylic acids around the QDs were determined as 1710 cm^{-1} and 1425 cm^{-1}. Finally, C-C stretching was found to be 1065 cm^{-1}. This information seems to be quite consistent when compared with the literature [30].

In the FTIR analysis of PVA/QDs nanocomposite structures, 670 cm^{-1} and 2956 cm^{-1} peaks of C-H peaks were found in all samples. When the intensity of the peaks was analyzed, it was determined that the peaks were stronger in PVA/QDs structures than in pure PVA. The main reason for this is the geometrically high tendency of C-H vibrations on a single surface [31]. Again, in PVA/QDs structures, 2875 cm^{-1} peaks were observed, which are not present in pure PVA nanocomposites and appear in the spectrum specific to QDs. Apart from this, when pure PVA nanocomposites and PVA/QDs nanocomposites are compared, it is seen that the OH peak of carboxylic acid at 3299 cm^{-1} and carbonyl peaks at 1682 cm^{-1} are stronger in pure PVA nanocomposites. The intensity of the C-C (1452 cm^{-1}) and C-O (1168 cm^{-1}) peaks also tended to be of the same strength. This is mainly due to the hydrogen bonding of OH and C-H groups in the PVA structure with MPA ligands and metallic interaction with the ligand of QDs [32].

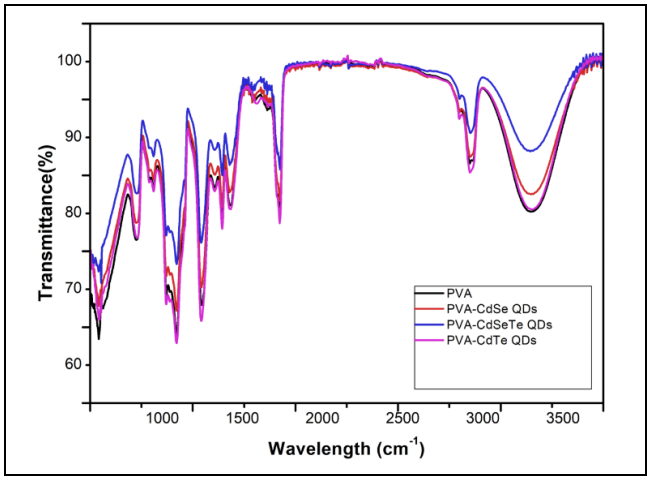

Figure 6. FT-IR Spectrum of PVA and Cd based Q. Dots -PVA nanocomposites.

UV-Vis absorption spectra of the samples in aqueous solution and thin films were performed using a Shimadzu UV-1800 ultraviolet visible spectrophotometer. The absorbance characterizations of the solvent and PVA matrix of the QDs synthesized in the study were performed and the results obtained are shown in Figure 7. The thickness of all surfaces tested in absorbance measurements was set to 0.15 mm so that each surface was considered equally.

The absorbance characterization results of PVA nanocomposites are shown in Figure 7(a). As can be seen, no absorbance peak was detected in the range of 400-750 nm for the PVA nanocomposite structure, with the known absorbance peak of PVA being 189 nm [33]. Figure 2(b) shows the absorbance characterization results of CdSe QDs dissolved in water and PVA/CdSe QDs nanocomposite. It was observed that the absorbance peak of the MPA-coated CdSe QDs synthesized here was at 493 nm, while the absorbance peak of the addition, the absorbance peaks of CdSe QDs in the PVA matrix lost their distinction, especially the second peak representing 2s2 transitions disappeared completely. It has been previously shown that the interaction of ligands on the surfaces of QDs and PVA matrix is different and this causes differences in the absorbance and emission characterization of the PVA/QDs structure [17]. This is thought to be mainly due to the interaction of the OH and C-H groups of the PVA matrix and the carboxyl groups in the MPA ligand used in all three QD types in this study. The PVA/QDs hybrid structure prepared at 60°C is thought to interact at the molecular level and cause shifts in absorbance peaks. Such shifts have been previously observed to occur in the absorbance peaks of QDs where similar processes were applied to treat the surface ligands [34]. The blue shift in PVA/CdSe QDs was similarly observed in PVA/CdTe QDs Figure 7(c) and PVA/CdTe QDs Figure 7(d) hybrid structures [35].

The energy band gap values of the synthesized QDs were calculated as 2.44 eV for CdSe QDs, 2.03 eV for CdTe QDs, and 2.06 eV for CdSeTe QDs [12]. The energy bandgap of the PVA/QDs nanocomposites structures was calculated using the absorbance spectrum according to the Tauc relation and shown in Figure 8.

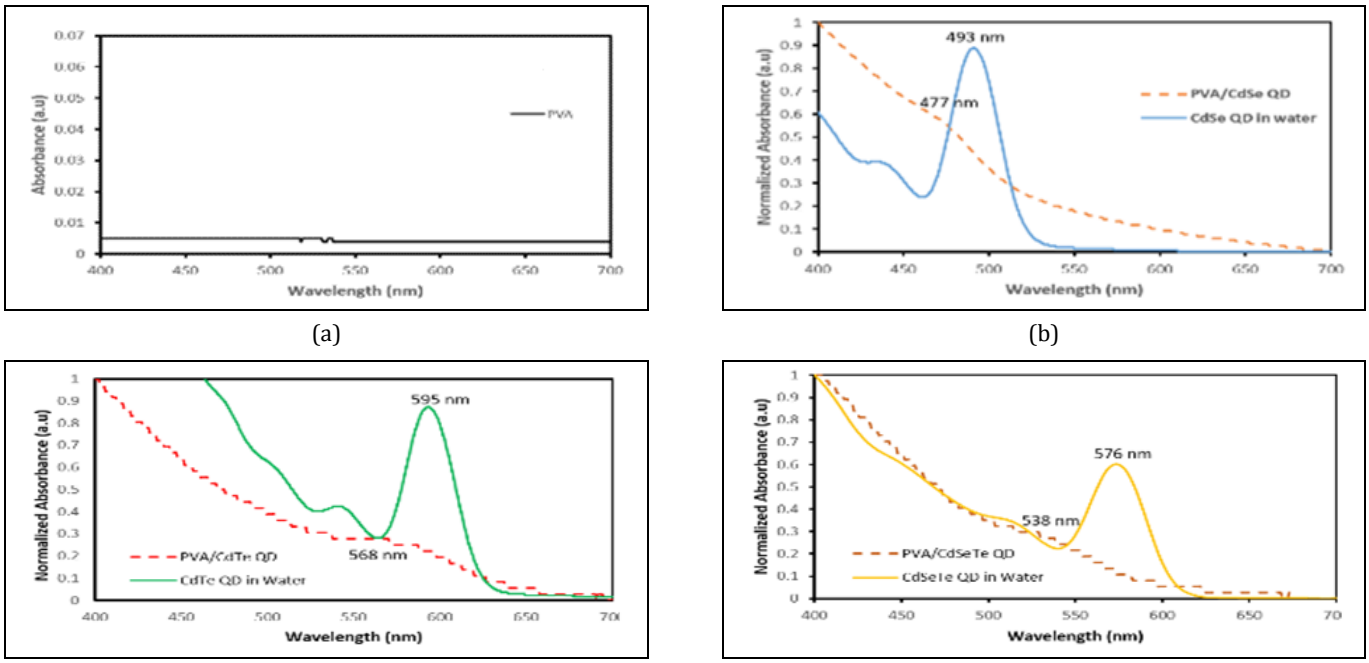

Figure 7. UV-Vis spectrum of Cd based QDs-PVA nanocomposites.

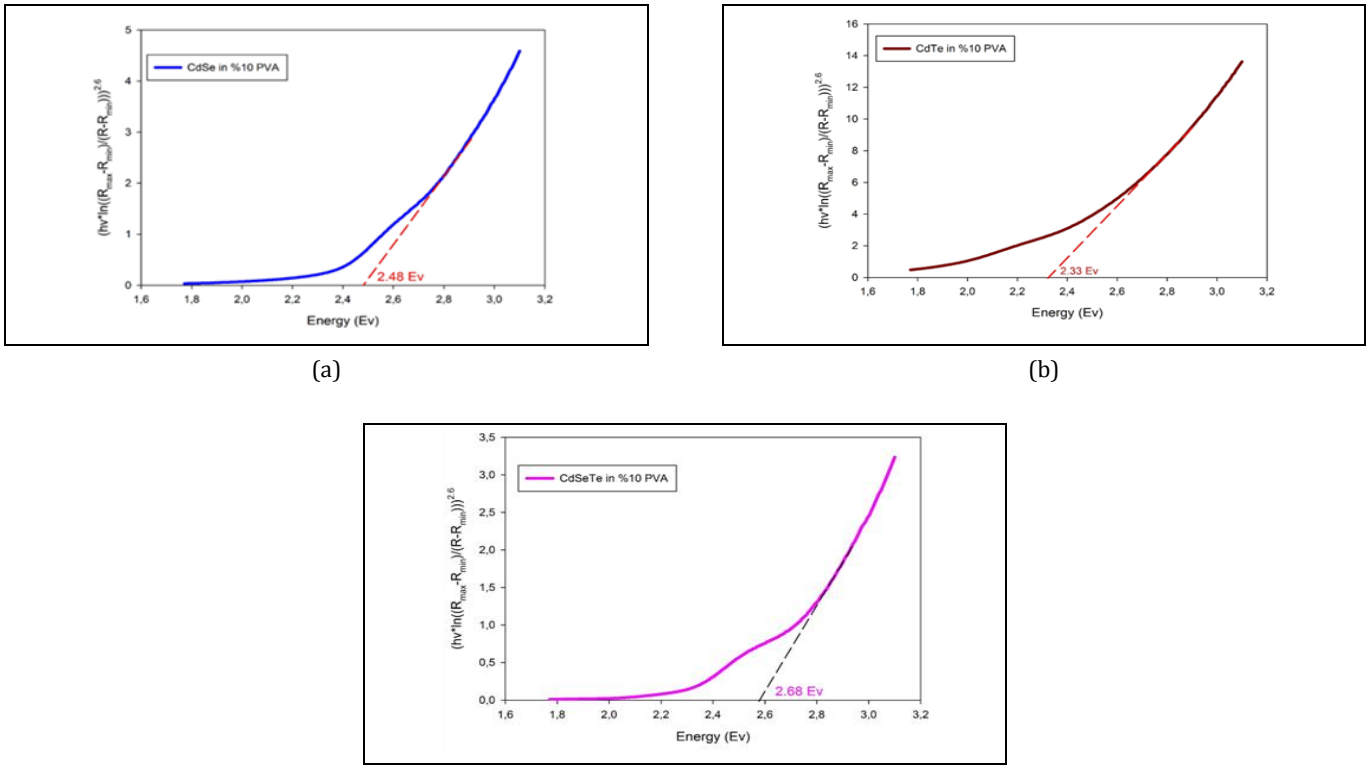

Figure 8. UV–Vis absorption to determine the bandgap of PVA-Cd Based QDs nanocomposites.

The Tauc relation is calculated from the formulas using a graph of ln {HV * ln [(R_{max}–R_{min}) /(R-R_{min})]} vs ln (hv-E_g). Using this formula and the absorbance measurements of the surfaces, the energy band gaps of the PVA/QDs structures were calculated. As a result of the calculations, energy band gaps of PVA/CdSe QDs, PVA/CdTe QDs, and PVA/CdSeTe QDs CdSe QD-PVA nanocomposites surfaces were found to be 2.48 eV, 2.33 eV, and 2.68 eV, respectively. The main difference between QDs (in water) and PVA/QDs is thought to be caused by the new hydrogen bond interactions between the carboxylic acid structures on the outermost surface of the QDs and PVA. This interaction is shown in Figure 8 as 2D interaction.

Figure 9 shows the fluorescence images and spectra of pure PVA, CdSe QDs, CdTe QDs, CdSeTe QDs and PVA/QDs nanocomposites. Edinburg FS5 fluorescence spectrometer was used for photoluminescence (PL) measurements and the excitation wavelength was selected as 383 nm for all surfaces. When the PL spectra results were analyzed, no significant fluorescence effect was observed in the 400-700 nm range of pure PVA nanocomposites as shown in Figure 9(a). On the other hand, it is known to have an emission peak around 340 nm due to the electronic* → n electronic transitions of -OH groups due to the spatial distribution of molecules in the PVA matrix [36]. On the other hand, the emission peaks of CdSe QDs, CdTe QDs and CdSeTe QDs used in this study vary depending on the synthesis time, and the emission peaks for the QDs used in this study were determined as 517 nm, 596 nm and 583 nm, respectively Figure 9(b)-(d). The emission characterizations obtained for these three QDs are in agreement with literature studies [37,38]. Although there were no emission peaks at 400-700 nm of the PVA matrix, emission peaks of PVA/QDs were observed with QDs added to the PVA matrix. Figure 9(b) shows that the peaks of PVA/CdSe QDs nanocomposites appear at 512 nm and have a blue shift of 5 nm compared to the emission peak of QDs in water.

Similarly, as shown in Figure 9(c), the emission peaks of PVA/CdTe QDs nanocomposites were observed at 593 nm with a blue shift of 3 nm. The amount of blue shift of the PVA/CdSeTe QDs nanocomposite structure reached 10 nm and the obtained emission characterizations are shown in Figure 9(d). The obtained results show that the OH groups in the PVA matrix, together with the QDs added to the PVA structure, cause the rearrangement of delocalized n groups [39]. One of the main reasons for the blue shift of the emission peaks of PVA/QDs nanocomposites relative to the emission peaks of QDs is thought to be due to the partial passivation of the surface traps of QDs by PVA-OH and COOH groups. A decrease in the strength of the emission peaks of PVA/QD nanocomposites in solvent was observed against the emission peaks of QDs. On the other hand, considering the emission of pure PVA, it is seen that the emission value of the PVA/QDs nanocomposite structure increases significantly with the addition of QDs. This is thought to be due to the electron capture ability of QDs in the PVA matrix and the increased recombination rate of electron-vacancy pairs.

Looking at the absorbance and emission characterization results given in Figure 8 and Figure 9, a red shift of the stoke is observed at the edges of the PVA/QDs emission band. Although this red shift in emission has been observed many times in the literature, it is attributed to the impurity of the structure, intermediates used, voids and surface defects [33].

3.2 Electrical Conductivity of PVA/QDs nanocomposites

The measurement results for the frequency-dependent electrical conductivity values of PVA/QDs whose composite structure is formed with CdSe QDs, CdTe QDs, and CdSeTe QDs are shown in Figure 10. In electrical conductivity measurements, while the frequency range was adjusted between 10 Hz. and 1 MHz, 2 V voltage was applied. Depending on the frequency, increases in the conductivity of nanocomposite materials have been observed. As can be seen from Figure 10, although it has been observed that the conductivity of nanocomposite materials consisting of PVA/CdSeTe QDs is the highest in all frequency ranges, it is observed that the addition of QDs provides extra electrical conductivity to PVA. The main reason for this increase in electrical conductivity is due to the conductive paths formed by the QDs within the PVA template [40].

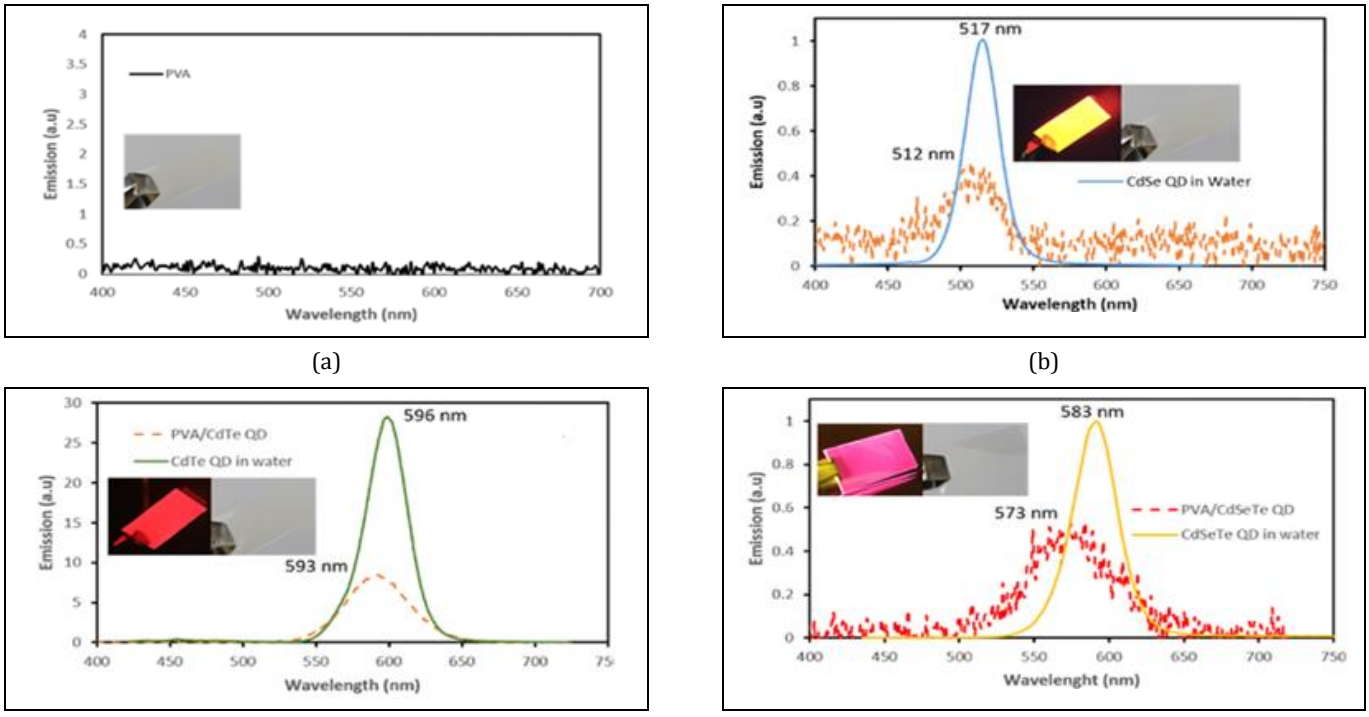

Figure 9. PL Spectrum of CdX QDs and CdX QDs-PVA nanocomposites.

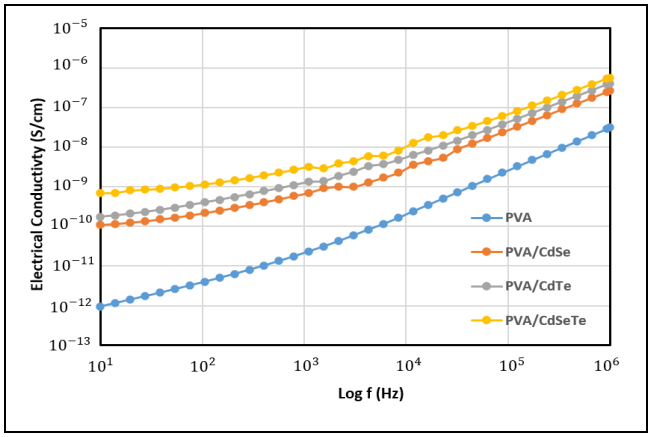

Figure 10. The electrical Conductivity of PVA/QDs nanocomposites depends on frequency.

Thanks to the conductivity channels produced by the QDs in the PVA matrix as an alternative, the charge transfer mechanism between the PVA and the QDs becomes operable, and the conductivity of the nanocomposite increases as the amount of charge carrier increases. In addition, due to the interaction of the MPA ligands coated on the surface of the QDs and the OH and COOH groups present in the PVA matrix, it is thought that the QDs are homogeneously distributed on the PVA surface and contribute to the increase of the surface conductivity.

When Figure 10 is examined, it is observed that the difference between the electrical conductivity of the QDs-added nanocomposites at low-frequency values and the electrical conductivity of the PVA polymer is more pronounced and this difference is up to 300 times, while at high-frequency values this difference tends to decrease. This is mainly since its conductivity is associated with the dielectric loss (ε''), which changes in ε'' depending on the frequency [41]. Similarly, it was determined that the conductivity values of the PVA/CdSeTe QDs nanocomposite structures showed better conductivity than the other two similar nanocomposites. In this case, it is thought that the synergetic effect of using Se^{2-} and Te^{2+} as a complex provides better conductivity than using these elements separately. Such that, as will be discussed in the next section, the ε'' values of PVA/CdSeTe QDs nanocomposites are higher than the other two counterparts.

3.3 Dielectric constant of PVA/QDs nanocomposites

The expression defining the complex dielectric constant which have real and imaginary parts can calculate with Equation 1 [40];

$$\varepsilon^{comp}(w) = \varepsilon'(w) - i\varepsilon''(w) \quad (1)$$

In this equation, the real part, ε', shows the dielectric constant, while $\varepsilon''$is the imaginary part, is the indicator of dielectric losses. To investigate the dielectric properties of PVA/QDs nanocomposites prepared by adding 3 different QDs were examined in the frequency range of 10 Hz - 1 MHz and the variation of dielectric constants depending on the frequency is shown in Figure 11.

The Dielectric constant is an indicator of a material's ability to polarize current electric dipoles against an electric field and to store energy [42].

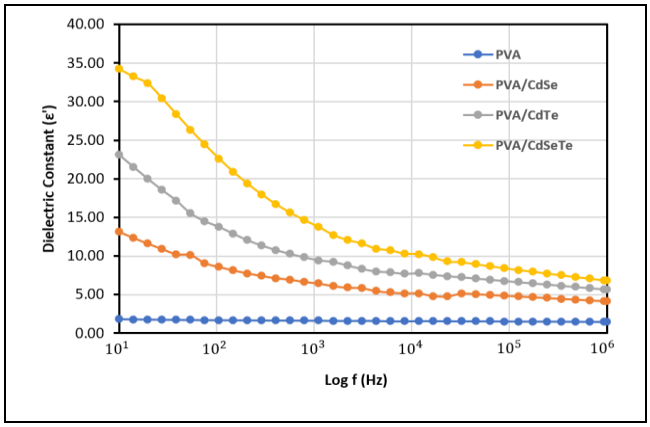

Figure 11. Variation of dielectric constants of nanocomposites concerning frequency.

The plot of the frequency-dependent dielectric constant for the PVA/QDs nanocomposite material with Figure 11 is compatible with the literature [43]. The initial ε'values are higher than the low-frequency values of polar materials. This is because the dipole moments in the existing nanocomposites have sufficient time to exhibit a structure that is compatible and aligned with the direction of the electric field at low frequency [44]. Compared to PVA, it has been observed that the ε' of PVA/QDs structures are quite high in the range of 10 Hz-10 kHz. On the other hand, with the increase in frequency, $\varepsilon'$of nanocomposites tended to decrease and the differences between ε'values gradually decreased. The decrease in ε' with increasing frequency basically does not provide enough time for the dipole moments to align in the direction of the electric field, which causes a decrease in polarization [45]. PVA is an insulating material, however, CdSe QDs, CdTe QDs, and CdSeTe QDs used in this study are semiconductor nanomaterials. Although this situation causes incompatibilities within the PVA/QDs nanocomposite material, the increase in dielectric constants of nanocomposite materials can be attributed to the QDs capacitors placed in the PVA matrix. Although the carboxyl groups on the surface of the QDs show good compatibility with the OH groups of PVA, they offer a harmonious dipolar interaction. As can be seen from Figure 11, it is seen that the addition of QDs increases the ' value. The dielectric constant of PVA/CdSeTe QDs has reached the highest value just like the electrical conductivity. This situation is thought to be caused by the harmony between the coated ligands on the surface of CdSeTe QDs and the surface of PVA, as well as the synergistic interaction of Se^{2-} and Te^{2+} at optimal values. Compared to CdSe QDs and CdTe QDs, alloy CdSeTe QDs are thought to be more efficient in bipolar interaction due to their higher capacitor properties within the PVA surface.

Dielectric Loss and Dissipation Factor (tan δ) of PVA/QDs nanocomposites

Dielectric losses and dissipation factor are related values. So that this can be represented by Equation 2 below;

$$\varepsilon'' = \varepsilon' \tan\delta \quad (2)$$

In this expression, tan δ shows the dissipation factor.

The variation of dielectric losses of PVA/QDs nanocomposites in the frequency range of 10 Hz - 1 MHz is given in Figure 12.

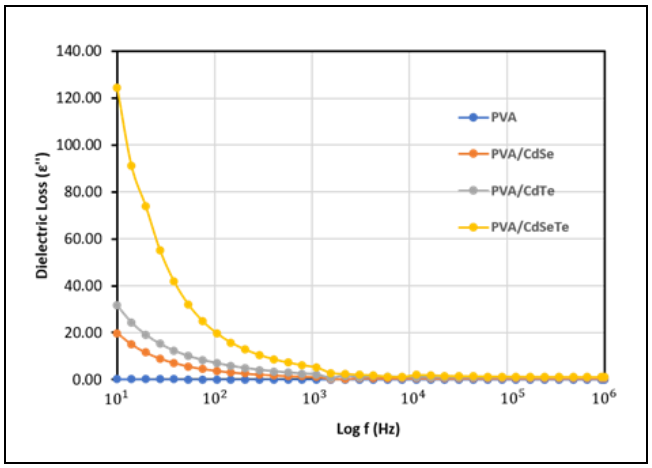

Figure 12. Variation of dielectric loss of PVA/QDs nanocomposites for frequency.

The dielectric loss of the nanocomposites was tested at room temperature at 2 Volt. As can be seen here, ε'' also varies significantly depending on the frequency. So much so that the increase in frequency causes a decrease in ε''. This situation is basically explained by the Waxwell-Warner model [46]. At low frequencies, as the PVA and QDs are not completely homogeneously distributed on the surface, interfacial polarization occurs with the electric field, which causes dielectric losses. On the other hand, the fluctuation in the electric field increases due to the increase in the frequency value, and in this case, the amount of polarization produced at the PVA/QDs interface is observed to below. This situation causes fewer dielectric losses in high-frequency ranges. When Figure 12 is examined, it is observed that dielectric losses in PVA/CdSeTe QDs are higher. This is basically due to similar reasons as the dielectric constant. CdSeTe QDs in PVA cause the formation of a conductive line on the PVA surface, which causes an increase in the charge transfer transitions occurring in the PVA matrix of CdSeTe QDs. This increase both the conductivity and dielectric losses of the composite structure. By the dielectric losses, the dissipation factor also changed depending on the frequency, and the results obtained are shown in Figure 13. As can be seen with Equation 1, the increase in dielectric losses causes an increase in tan δ. Similarly, the decrease in dielectric losses depending on the frequency causes a decrease in tan δ.

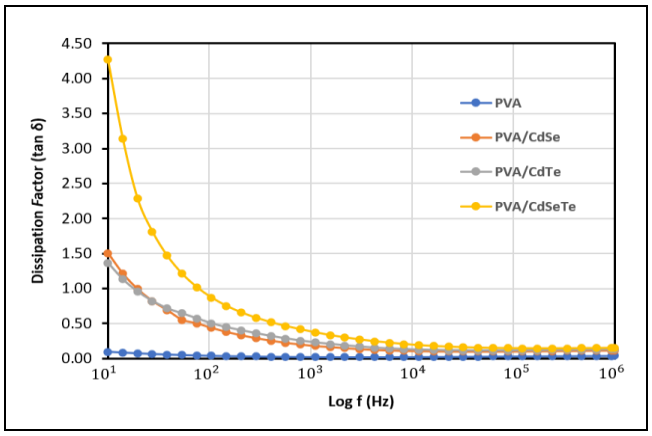

Figure 13. Variation of dissipation factor of PVA/QDs nanocomposites for frequency.

4 Conclusions

In this study, Cd-based QDs-PVA nanocomposite structures were formed by adding 3 different Cd-based QDs to the PVA matrix. The morphological, thermal, optical, photoluminescence and electrical properties of PVA/QDs nanocomposite structures were investigated. The ionic interactions between PVA matrix, CdSe QDs, CdTe QDs and CdSeTe QDs were investigated. In all PVA/QDs nanocomposite structures formed in the study, it was observed that QDs were homogeneously dispersed in the PVA matrix and results were obtained according to the optical properties of QDs in both absorbance and emission characterizations. On the other hand, QDs dispersed in PVA matrix were found to have blue shifts in absorbance and emission peaks due to the interactions between hydroxyl groups and OH and COOH groups in MPA ligands. While all QDs added to the PVA matrix caused an increase in the fluorescence of PVA, the highest fluorescence increase occurred with the addition of CdSeTe QDs. No significant difference was detected when the morphological properties of PVA/QDs were analyzed. It was observed that all three PVA/QDs nanocomposite structures were compatible with the Zinc Blende Cubic structure (crystal structure of QDs). No major differences were observed in the SEM images of the surfaces. However, when the thermal properties of PVA/QDs were examined, increases in the thermal decomposition temperatures and melting points of the nanocomposites were observed with the addition of QDs to the PVA matrix. The data obtained at this stage showed that the alloy structure and CdSeTe QDs gave better results in both degradation temperatures and melting point increase in PVA matrix compared to QD types. Finally, when the impedance values of PVA/QDs nanocomposites are compared with pure PVA nanocomposites, increases in dielectric constants and conductivity are observed. In fact, when CdSe QDs and CdTe QDs were added to the PVA matrix, the conductivity of the surface increased 100 times. However, with the addition of CdSeTe QDs, the conductivity was increased up to 1000 times. In conclusion, in this study where three different QDs were tested in PVA matrix, CdSeTe QDs were found to be more effective than CdSe QDs and CdTe QDs in both thermal and conductivity properties of PVA. As a result of the study, it is predicted that the hybrid organic/inorganic structure of PVA/QDs can be used for application in light emitting devices and has a high potential for biomedical research.

5 Author contribution statements

The authors confirm their contribution to the paper as follows: Tuna DEMİRCİ designed and performed the experiments, and analyzed the data. Erdem ELİBOL supervised the study and contributed to the design and implementation of the research. Şeref KARADENİZ aided in interpreting the results and worked on the manuscript. All authors discussed the results and commented on the manuscript.

6 Ethics committee approval and conflict of interest statement

"There is no need to obtain permission from the ethics committee for the article prepared".

"There is no conflict of interest with any person / institution in the article prepared".

7 Reference

[1] Nozik AJ, Beard MC, Luther JM, Law M, Ellingson RJ, Johnson JC. "Semiconductor quantum dots and quantum dot arrays and applications of multiple exciton generation to third-generation photovoltaic solar cells". *Chemical Reviews*, 110(11), 6873-6890, 2010.

[2] Murray CB, Norris DJ, Bawendi MG. "Synthesis and characterization of nearly monodisperse CdE (E=sulfur, selenium, tellurium) semiconductor nanocrystallites". *Journal of the American Chemical Society*, 115(19), 8706-8715, 1993.

[3] Zhao L, Hu L, Fang X. "Growth and Device Application of CdSe Nanostructures". *Advanced Functional Materials*, 22(8), 1551-1566, 2012.

[4] Choi Y, Seol M, Kim W, Yong K. "Chemical Bath Deposition of Stoichiometric CdSe Quantum Dots for Efficient Quantum-Dot-Sensitized Solar Cell Application". *The Journal of Physical Chemistry*, 118(11), 5664-5670, 2014.

[5] Zou G, Ju H. "Electrogenerated Chemiluminescence from a CdSe Nanocrystal Film and Its Sensing Application in Aqueous Solution". *Analytical Chemistry*, 76(23), 6871–6876, 2004.

[6] Sun X, Huang X, Guo J, Zhu W, Ding Y, Niu G. "Self-Illuminating 64 Cu-Doped CdSe/ZnS Nanocrystals for in Vivo Tumor Imaging". *Journal of the American Chemical Society*, 136(5), 1706-1709, 2014.

[7] Tiwari D, Tanaka S-I, Inouye Y, Yoshizawa K, Watanabe T, Jin T. "Synthesis and characterization of Anti-HER2 antibody conjugated CdSe/CdZnS quantum dots for fluorescence ımaging of breast cancer cells". *Sensors*, 9(11), 9332-9354, 2009.

[8] Kaur R, Tripathi SK. "Study of conductivity switching mechanism of CdSe/PVP nanocomposite for memory device application". *Microelectronic Engineering*, 133, 59-65, 2015.

[9] Handique KC, Kalita PK. "Effects of cadmium ion concentration on the optical and photo-response properties of CdSe/PVP nanocomposites for white light sensing application". *Applied Physics A: Materials Science & Processing*, 126(9), 1-12, 2020.

[10] Sun H, Wu P. "Tuning the functional groups of carbon quantum dots in thin film nanocomposite membranes for nanofiltration". *Journal of Membrane Science*, 564, 394-403, 2018.

[11] Qaid SMH, Al-Asbahi BA, Ghaithan HM, AlSalhi MS, Al Dwayyan AS. "Optical and structural properties of $CsPbBr_3$ perovskite quantum dots/PFO polymer composite thin films". *Journal of Colloid and Interface Science*, 563, 426-434, 2020.

[12] Suo B, Su X, Wu J, Chen D, Wang A, Guo Z. "Poly (vinyl alcohol) thin film filled with CdSe–ZnS quantum dots: Fabrication, characterization and optical properties". *Materials Chemistry and Physics*, 119(1–2), 237-242, 2010.

[13] Fritz KP, Guenes S, Luther J, Kumar S, Sariciftci NS, Scholes GD. "IV–VI Nanocrystal–polymer solar cells". *Journal of Photochemistry and Photobiology A: Chemistry*, 195(1), 39-46, 2008.

[14] Murria M, Sharma RK, Mehta C. "Capacitance-voltage profiling of aluminium junctioned PVA/CdSe nanocomposite schottky diode". *Materials Today: Proceedings*, 28, 1445-1449, 2020.

[15] Patil AS, Waghmare RD, Pawar SP, Salunkhe ST, Kolekar GB, Sohn D. "Photophysical insights of highly transparent, flexible and re-emissive PVA @ WTR-CDs composite thin films: A next generation food packaging material for UV blocking applications". *Photochemistry and Photobiology A: Chemistry*, 400, 112647-112656, 2020.

[16] Oliveira E, Santos HM, Jorge S, Rodríguez-González B, Novio F, Lorenzo J. "Sustainable synthesis of luminescent CdTe quantum dots coated with modified silica mesoporous nanoparticles: Towards new protein scavengers and smart drug delivery carriers". *Dyes and Pigments*, 16, 360-369, 2019.

[17] Barandiaran I, Gutierrez J, Etxeberria H, Tercjak A, Kortaberria G. "Tuning photoresponsive and dielectric properties of PVA/CdSe films by capping agent change". *Composites Part A: Applied Science and Manufacturing*, 118, 194-201, 2019.

[18] Yang Q, Tang K, Wang C, Qian Y, Zhang S. "PVA-Assisted Synthesis and Characterization of CdSe and CdTe Nanowires". *The Journal of Physical Chemistry B*, 106(36), 9227-9230, 2002.

[19] Elibol E. "Synthesis of near unity photoluminescence CdSeTe alloyed Quantum Dots". *Journal of Alloys and Compounds*, 817, 152726-152737, 2020.

[20] Marc C, Catherine LV, Wilms EB, Brigitte E, Frédéric C, Mircea A, Didier L. "A Novel Cross-linked Poly(vinyl alcohol) (PVA) for Vascular Grafts". *Composites Part B: Engineering*, 250, 110456, 2023.

[21] Moises B, David R, Belén A, Kenia P, Héctor M, Emilio B. "Hydrogels classification according to the physical or chemical ınteractions and as stimuli-sensitive materials". *Gels*, 7(4), 182, 2021.

[22] Hamizi NA, Johan MR. "Synthesis and size dependent optical studies in CdSe quantum dots via inverse micelle technique". *Materials Chemistry and Physics*, 124(1), 395–398, 2010.

[23] Elibol E, Tutkun N. "Improving CdTe QDSSC's performance by Cannula synthesis method of CdTe QD". *Materials Science in Semiconductor Processing*, 93, 304-316, 2019.

[24] Elibol E. "Quantum dot sensitized solar cell design with surface passivized CdSeTe QDs". *Solar Energy*, 206, 741-750, 2020.

[25] Hoang QB, Mai VT, Nguyen DK, Truong DQ, Mai XD. "Crosslinking induced photoluminescence quenching in polyvinyl alcohol-carbon quantum dot composite". *Materials Today Chemistry*, 12, 166-172, 2019.

[26] Kyobe JW, Khan MD, Kinunda G, Mubofu EB, Revaprasadu N. "Synthesis of CdTe quantum dots capped with castor oil using a hot injection solution method". *Materials Science in Semiconductor Processing,* 106, 104780-104787, 2020.

[27] Elibol E, Demirci T. "Performance analysis of hybrid quantum dots sensitized solar cells consisting of CdS/CdX (X = Se, Te, SeTe) QD and bromophenol blue dye". *Optical Materials*, 122, 111785-111799, 2021.

[28] Hellwig P, Rost B, Kaiser U, Ostermeier C, Michel H, Mäntele W. "Carboxyl group protonation upon reduction of the Paracoccus denitrificans cytochrome c oxidase: direct evidence by FTIR spectroscopy". *FEBS Letters*, 29, 385(1–2), 53-57, 1996.

[29] Deschenaux C, Affolter A, Magni D, Hollenstein C, Fayet P. "Investigations of CH4, C2H2 and C2H4 dusty RF plasmas by means of FTIR absorption spectroscopy and mass spectrometry". *Journal of Physics D: Applied Physics*, 32(15), 1876-1886, 1996.

[30] Elibol E, Demirci T. "An Investigation the spectroscopic charactarization of alloy CdSeTe quantumdots/ bromophenol blue hybrid associates". *Sakarya University Journal of Science*, 25(1), 200-211, 2020.
[31] Cao L, Tang F, Fang G. "Preparation and characteristics of microencapsulated palmitic acid with TiO2 shell as shape-stabilized thermal energy storage materials". *Solar Energy Materials and Solar Cells*, 123, 183-188, 2014.
[32] Sabah A, Tasleem S, Murtaza M, Nazir M, Rashid F. "Effect of polymer capping on photonic multi-core–shell quantum dots CdSe/CdS/ZnS: Impact of sunlight and antibacterial activity". *The Journal of Physical Chemistry*, 124(16), 9009-9020, 2020.
[33] Rahman KMM, Pal S, Hoque MM, Alam MR, Younus M, Kobayashi H. "Simple fabrication of PVA-ZnS composite films with superior photocatalytic performance: enhanced luminescence property, morphology, and Thermal Stability". *ACS Omega*, 4(4), 6144-6153, 2019.
[34] Elibol E, Elibol PS, Cadırcı M, Tutkun N. "Improving the performance of CdTe QDSSCs by chloride treatment and parameter optimization". *Materials Science in Semiconductor Processing,* 96, 30-40, 2019.
[35] Borkovska L, Korsunska N, Stara T, Gudymenko O, Venger Ye, Stroyuk O." Enhancement of the photoluminescence in CdSe quantum dot–polyvinyl alcohol composite by light irradiation". *Applied Surface Science*, 281, 118-122, 2013.
[36] Ram S, Mandal TK. "Photoluminescence in small isotactic, atactic and syndiotactic PVA polymer molecules in water". *Chemical Physics*, 303(1–2), 121-128, 2004.
[37] Azpiroz JM, de Angelis F. "Ligand ınduced spectral changes in cdse quantum dots". *ACS Applied Materials & Interfaces*, 7(35), 19736–19745, 2015.
[38] Elibol E, Elibol PS, Çadırcı M, Tutkun N. "Improved photoluminescence and monodisperse performance of colloidal CdTe quantum dots with Cannula method". *Korean Journal of Chemical Engineering*, 36(4), 625-634, 2019.
[39] Dey KK, Kumar P, Yadav RR, Dhar A, Srivastava AK. "CuO nanoellipsoids for superior physicochemical response of biodegradable PVA". *RSC Advances*, 4(20), 10123, 2014.
[40] El-Shamy AG, Zayied HSS. "New polyvinyl alcohol/carbon quantum dots (PVA/CQDs) nanocomposite films: Structural, optical and catalysis properties". *Synthetic Metals*, 259, 116218-116232, 2020.
[41] Malik P, Chaudhary A, Mehra R, Raina KK. "Electrooptic and dielectric studies in cadmium sulphide nanorods/ferroelectric liquid crystal mixtures". *Advances in Condensed Matter Physics*, 2012, 1-8, 2017.
[42] ripathi PK, Pande M, Singh S. "Dielectric and electro-optical properties of polymer-stabilized liquid crystal. II. polymer PiBMA dispersed in MBBA". *Applied Physics A*, 122(9), 847-857, 2016.
[43] Heiba ZK, Mohamed MB, Imam NG, Mostafa NY. "Optical and electrical properties of quantum composite of polyvinyl alcohol matrix with CdSe quantum dots". *Colloid and Polymer Science*, 294(2), 357-365, 2016.
[44] El-Shamy AG, Maati AA, Attia W, Abd El-Kader KM. "Promising method for preparation the PVA/Ag nanocomposite and Ag nano-rods". *Journal of Alloys and Compounds*, 744, 701-711, 2018.
[45] Kocakülah G, Algül G, Köysal O. "Effect of CdSeS/ZnS quantum dot concentration on the electro-optical and dielectric properties of polymer stabilized liquid crystal". *Journal of Molecular Liquids*, 299, 112182-112190, 2020.
[46] Thomassin JM, Jérôme C, Pardoen T, Bailly C, Huynen I, Detrembleur C. "Polymer/carbon-based composites as electromagnetic interference (EMI) shielding materials". *Materials Science and Engineering: R: Reports*, 74(7), 211-232, 2013.